Vibronic Absorption Spectra of Naturally Occurring Conjugated Polyenynes. Evidence for Localized Excitations

Giulietta Smulevich * **and Mario P. Marzocchi**
Dipartimento di Chimica dell'Università, Via G. Capponi 9, 50121 Firenze, Italy
Franco F. Vincieri, Silvia A. Coran, and Massimo Bambagiotti Alberti
Dipartimento di Scienze Farmaceutiche dell'Università, Via G. Capponi 9, 50121 Firenze, Italy

The second-derivative technique has been used to measure the absorption spectra of a series of related naturally occurring polyenynes whose chromophoric fragments range from three to six conjugated groups. The reliability of the second-derivative method has been checked by comparison between the observed and calculated absorption and second-derivative spectra in terms of the vibronic theory. The spectral resolution achieved allowed the vibrational structure of the electronic transitions to be analysed. This is useful in identifying the chromophore involved in the electronic excitation. The spectra have been interpreted in terms of localized excitons and subsequent excitation transfer. These results account for the structural characteristics, stereoisomerism included, of a given sequence of triple and double bonds providing a complete fingerprint of the polyenyne chromophore.

The electronic spectra of linear polyenes have been studied in terms of MO theory.[1] However, simple treatment, neglecting electron correlations, fails to predict the bond length alternation of single and double bonds[2] as well as the spectral convergence of the observed low lying strong band to a constant frequency as the chain length tends towards large values.[3] In addition the presence of a low lying A_g (C_{2h} symmetry) state cannot be explained.[1] All these observations have been interpreted in terms of the SFC method including configuration interaction with single and double excited states or by the valence bond treatment.[4]

Calculations of the electronic spectra of linear polyenes based on the exciton model in which the double bonds are treated as quasi-independent weakly interacting systems have been performed,[5–9] leading to good agreement with experiment. Also the A_g excited state has been simply accounted for by the exciton picture, once double excitation to the triplet states of two different units is considered.[10]

In this paper we show that the electronic spectra of conjugated chromophores can be easily interpreted in terms of localized excitons, the interaction between the units involving electron or exciton transfer. We have taken advantage of the availability of a series of naturally occurring polyenynes[11,12] exhibiting slightly different conjugated double and triple carbon bonds. We observed resolved spectra by the second-derivative (D^2) technique. Analysis of the vibrational structure of the electronic transitions is very helpful in identifying the chromophore involved in the electronic excitation.

Even if higher resolution could be achieved by low-temperature spectra, we think that such measurements are not necessary for our purpose. We want (i) to characterize the specific chromophore involved in a given electronic excitation, (ii) to furnish a simple method for the qualitative interpretation of the u.v.–visible electronic transitions for each compound, and (iii) to explore the possibility of obtaining the type, position, and configuration of the non-aromatic unsaturated groups in an unknown complex molecule.

Experimental

Pentadeca-*trans*-2,*cis*-9-diene-4,6-diyne (**I**), pentadeca-*trans*-2-ene-4,6-diyn-10-one (**II**), pentadeca-*trans*-2,*trans*-8-diene-4,6-diyn-12-one (**III**), pentadeca-*trans*-2,*trans*-8-diene-4,6-diyn-10-ol (**IV**), pentadeca-*trans*-2,*trans*-8,*trans*-10-triene-4,6-diyne (**V**), pentadeca-*trans*-2,*trans*-8,*trans*-10-triene-4,6-diyn-12-ol (**VI**), pentadeca-*trans*-2,*trans*-8,*cis*-10-triene-4,6-diyne (**VII**), pentadeca-*trans*-2,*cis*-8,*trans*-10-triene-4,6-diyne (**VIII**), pentadeca-*trans*-2,*cis*-8,*trans*-10-triene-4,6-diyn-12-ol (**IX**), pentadeca-*trans*-2,*cis*-8,*cis*-10-triene-4,6-diyne (**X**), pentadeca-*trans*-2,*trans*-8-diene-4,6-diyn-10-one (**XI**), pentadeca-*trans*-2,*trans*-8,*trans*-10-triene-4,6-diyn-12-one (**XII**), and pentadeca-*trans*-2,*cis*-8,*trans*-10-triene-4,6-diyn-12-one (**XIII**) were all extracted from *Oenanthe aquatica* fruits, isolated, and purified as previously described.[11,12]

Normal and D^2 u.v. spectra, in n-hexane, were recorded on a Perkin-Elmer 552/S spectrophotometer in 1 cm path low-volume cell. D^2 Spectra were run at 120 nm min^{-1} scan speed, 1 nm slit width, and 0.5 s response.

In order to check the effect of distortion from noise, the absorption and second-derivative spectra of compounds (**I**) and (**X**) were also recorded on a Perkin-Elmer Lambda 9 spectrometer, at various scan speeds ranging from 30 to 240 nm min^{-1} and various $\Delta\lambda$ values ranging from 1 to 8 nm (the instrument approximates to the second derivative at some particular wavelength λ' according to $(d^2A/d\lambda^2)_{\lambda'} = [(A_{\lambda'+\Delta\lambda} - 2A_{\lambda'} + A_{\lambda'+\Delta\lambda})/(\Delta\lambda)^2]$.

Results and Discussion

Figures 1—5 show the absorption spectra,[13] together with the corresponding second-derivative spectra, of various naturally occurring substituted polyenynes whose chromophoric fragments range from three to six conjugated unsaturated groups. It is seen that the spectra display numbers of peaks which take their origins from various electronic transitions with their vibrational structures.

In order to interpret the spectra we take into account the following points. (1) Each $\pi \longrightarrow \pi^*$ allowed transition is quasi-localized to a single group (ethylene, acetylene, carbonyl). (2) Two equal adjacent chromophores give rise to exciton splitting into two components of the double degenerate excited state. (3) The relative intensities of the two components are roughly predicted on the basis of the pseudo-symmetry (the extent of the distortion from the C_{2h} symmetry) of the double chromophore. (4) The number of the expected transitions is equal to the number of conjugated π bonds. (5) The wavelengths of the purely electronic transitions are related to the long-wavelength band of the series of the conjugated polyenes $H{-}(CH{=}CH)_n{-}H$,

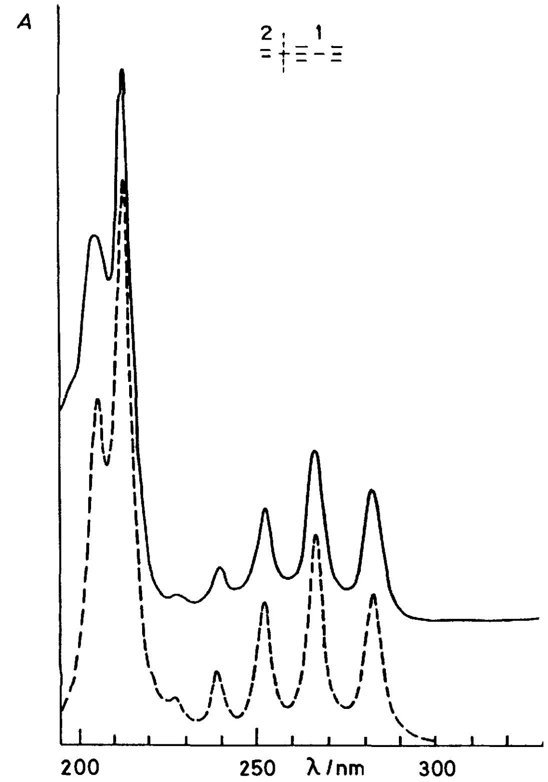

Figure 1. Experimental (——) and calculated (– – –) according to equation (1) (see text) absorption spectra of pentadeca-*trans*-2,*cis*-9-diene-4,6-diyne in n-hexane. Experimental conditions: scan speed 60 nm min^{-1}, response 0.5 s, slit width 1 nm

polyynes CH_3–$(C{\equiv}C)_n$–CH_3, and polyene aldehydes CH_3–$(CH{=}CH)_n$–CHO.[14] (6) The vibrational structures of all the transitions are essentially characterized by the carbon–carbon (or carbon–oxygen) stretching modes. It has been observed in absorption and resonance Raman spectra of various unsaturated hydrocarbons (see for example refs. 15 and 16) that the C=C and C–C stretching modes give rise to by far the strongest bands. (7) All the electronic transitions are $\pi \longrightarrow \pi^*$ Franck–Condon allowed. The relative intensities of the vibrational components are therefore given in terms of Δ, the potential curve shift of each mode between the ground and the excited state.[17] (8) The vibrational structure of each electronic transition has been detected by means of the second-derivative method. In order to ensure that the D^2 technique furnishes sufficient resolution without producing band distortion or false peaks we have performed a detailed analysis, both experimental and theoretical, of the D^2 spectrum of the simplest compound (**I**). We measured the spectrum under various conditions changing the scan speed, Δλ, and the slit width. We also calculated both the absorption and its D^2 spectra in terms of the vibronic theory by using the same parameters. The aim of this calculation is to find an analytical function, in terms of a sum of Lorentzian curves, which fits the experimental absorption spectrum and can be easily adapted to fit the experimental second-derivative spectrum.

The spectral absorbance $A(\nu)$ is given by equation (1) where

$$A(\nu) = K\nu\left[M_1^2\sum_{v_3}\frac{\langle v_3|0\rangle^2\,\Gamma_{1v}}{(\nu_{00_1} + v_3\nu_3 - \nu)^2 + \Gamma_{1v}^2} + M_2^2\sum_{v_2}\sum_{v_3}\frac{\langle v_2|0\rangle^2\,\langle v_3|0\rangle^2\,\Gamma_{2v}}{(\nu_{00_2} + v_2\nu_2 + v_3\nu_3 - \nu)^2 + \Gamma_{2v}^2}\right] \quad (1)$$

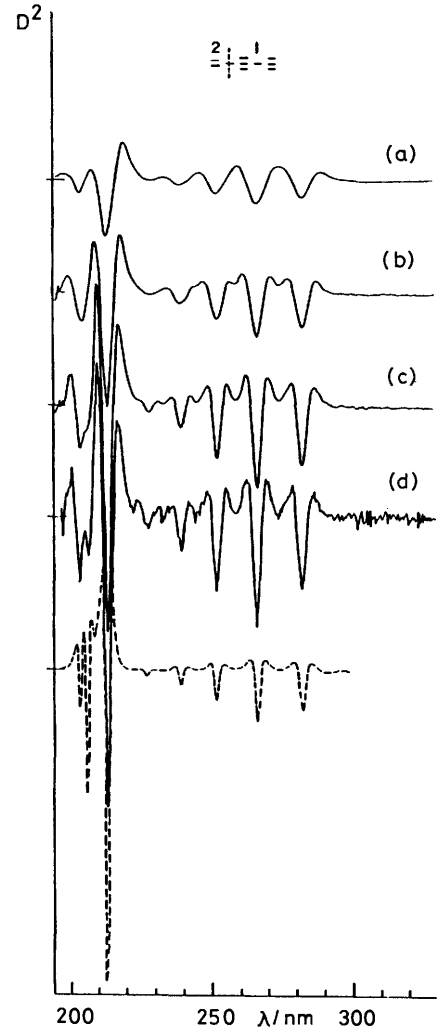

Figure 2. Experimental (——) and calculated (– – –) according to equation (4) (see text) second-derivative spectra of pentadeca-*trans*-2,*cis*-9-diene-4,6-diyne in n-hexane. Experimental conditions as Figure 1; (a), Δλ 6; (b), Δλ 4; (c), Δλ 2; (d), Δλ 1 nm

M_1 and M_2 are the transition moments of the S_0–S_{1B} and S_0–S_2 transitions whose origins are located at ν_{00_1} 35 587 cm^{-1} (281 nm) and ν_{00_2} 47 281 cm^{-1} (211.5 nm); ν_2 and ν_3 are the frequencies of the $\nu_{C=C}$ and $\nu_{C\equiv C}$ modes at 1 600 and 2 140 cm^{-1}, respectively; v_2 and v_3 are the corresponding vibrational quantum numbers, their sum truncated for $v_2,v_3 \leqslant 1$ for the transition S_0–S_2 and $v_3 \leqslant 5$ for the transition S_0–S_{1B}. The damping factors Γ_{1v} 350 cm^{-1} and Γ_{2v} 600 cm^{-1} are assumed to be equal for all the vibrational terms of the same electronic transition; the spectral frequency ν ranges from 33 333 (300) to 51 020 cm^{-1} (196 nm). $\langle v_i|0\rangle$ are vibrational overlap integrals such that the relative intensity I of each vibronic band to the intensity I_0 of the electronic origin is given by equation (2) for

$$I_{0-v_i}/I_{0-0} = \langle v_i|0\rangle^2/\langle 0|0\rangle^2 = (\Delta_i^2/2)^{v_i}/v_i\,! \quad (2)$$

fundamentals and overtones and equation (3) for combinations

$$I_{0-v_i+v_j}/I_{0-0} = \langle v_i|0\rangle^2\,\langle v_j|0\rangle^2/\langle 0|0\rangle^2 = (\Delta_i^2/2)^{v_i}/v_i\,! \times (\Delta_j{}^2/2)^{v_j}/v_j\,! \quad (3)$$

where $\langle 0|0\rangle^2 = \exp(-\tfrac{1}{2}\Delta_i^2 - \tfrac{1}{2}\Delta_j^2)$ and Δ_i,Δ_j are the potential curve shift along the normal co-ordinate between the ground and the excited states. Their values have been estimated from the maximum intensities of both experimental absorption and second-derivative spectra [equation (2)]. $\Delta_3 = 1.6$ and 0.6 for S_0–S_{1B} and S_0–S_2 electronic transitions respectively and $\Delta_2 = 0.9$.

The intensity $A(\nu)$ has been normalized with the scale factor $K = 0.6$ to the intensity of the origin of the S_0–S_{1B} transition. The ratio $M_2^2 \langle 0|0\rangle_2^2 / M_1^2 \langle 0|0\rangle_1^2 = A = 8$ has been estimated from the intensity ratio of the two electronic transitions.

The second derivative of the analytical function $A(\nu)$ is given by equation (4).

Figure 1 shows the comparison between the observed and calculated absorption spectra. It is seen that the agreement is very good apart from the region below 200 nm. The discrepancy is accounted for by neglecting the contributions of the higher vibrational terms of the S_0–S_2 transition and the probable occurrence of a third weak electronic transition.

Figure 2 shows the measured D^2 spectra at various $\Delta\lambda$ values and the calculated $d^2A(\lambda)/d\lambda^2$ spectrum by using the $A(\lambda)$ function [equation (1)] [$A(\nu)$ is easily transformed into $A(\lambda)$]. Also in this case the agreement between the experimental and calculated curves is fairly good if the instrumental limit due to the finite $\Delta\lambda$ is considered. It is seen that the band widths decrease and the intensity increases in absolute value when $\Delta\lambda$ decreases. At $\Delta\lambda$ 1, the minimum available instrumental value, the peaks are rather sharp, but the signal-to-noise ratio is weak.

$$
\begin{aligned}
d^2A(\nu)/d\nu^2 = {} & K\sum_{v_3}\frac{\langle v_3|0\rangle^2}{\langle 0|0\rangle^2} \times \left\{\frac{-2\nu}{[(\nu_{00_1} + v_3\nu_3 - \nu)^2 + \Gamma_{1v}^2]^2} + \frac{4(\nu_{00_1} + v_3\nu_3 - \nu)\,[(\nu_{00_1} + v_3\nu_3)^2 + \Gamma_{1v}^2 - \nu^2]}{[(\nu_{00_1} + v_3\nu_3 - \nu)^2 + \Gamma_{1v}^2]^3}\right\} + \\
& KA\sum_{v_2}\sum_{v_3}\frac{\langle v_3|0\rangle^2 \langle v_2|0\rangle^2}{\langle 0|0\rangle^2} \times \left\{\frac{-2\nu}{[(\nu_{00_2} + v_2\nu_2 + v_3\nu_3 - \nu)^2 + \Gamma_{2v}^2]^2} + \right. \\
& \left. \frac{4(\nu_{00_2} + v_2\nu_2 + v_3v_3 - \nu)\,[(\nu_{00_2} + v_2\nu_2 + v_3\nu_3)^2 + \Gamma_{2v}^2 - \nu^2]}{[(\nu_{00_2} + v_2\nu_2 + v_3\nu_3 - \nu)^2 + \Gamma_{2v}^2]^3}\right\} \qquad (4)
\end{aligned}
$$

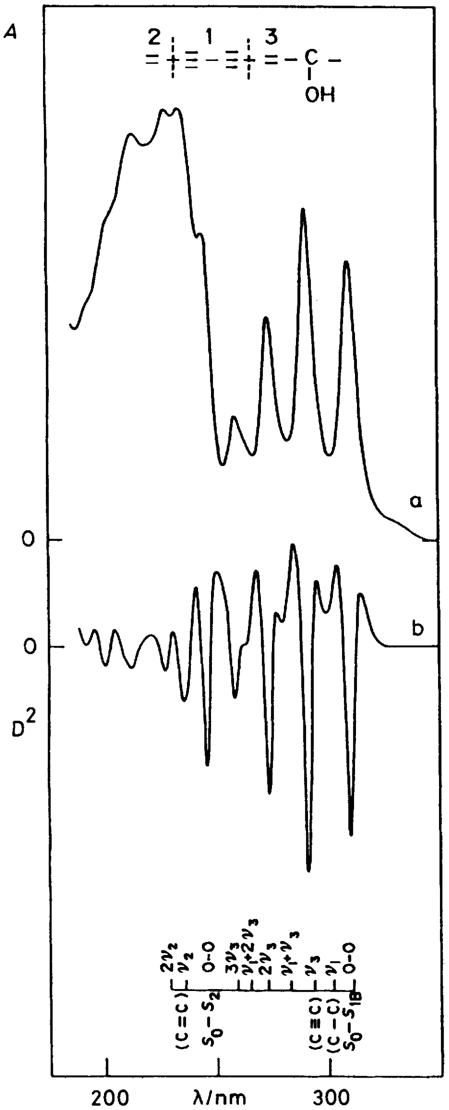

Figure 3. Absorption (a) and second-derivative spectra (b) of pentadeca-*trans*-2,*trans*-8-diene-4,6-diyn-10-ol in n-hexane. The vibrational assignment of the highest-wavelength transition is indicated

The calculated D^2 spectrum should be considered to be the extrapolated one at $\Delta\lambda \longrightarrow 0$. Comparison among the strong peaks of the D^2 spectra clearly leads to the conclusion that they are highly reliable at sufficient resolution. Bands spaced as much as 2 nm apart at 200 nm (see the spacing between the $\nu_{C\equiv C}$ and $v_{C\!=\!C}$ modes of the S_0–S_2 transition observed in both the experimental and calculated D^2 spectra) or less can be easily detected with no distortion either in maximum wavelengths or intensities (the estimated error in $\lambda_{max.}$ is ±0.5 nm).

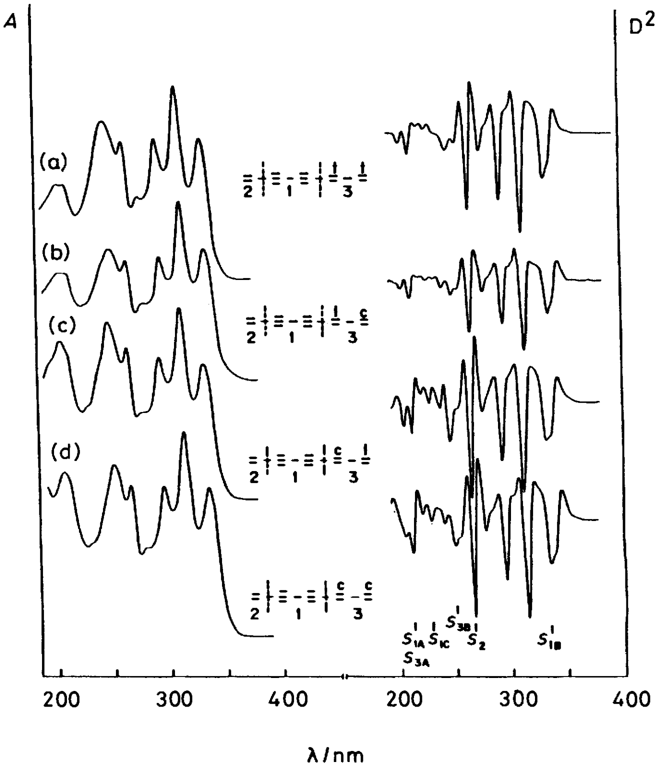

Figure 4. Absorption (left) and second-derivative (right) spectra of pentadeca-*trans*-2,*trans*-8,*trans*-10-triene-4,6-diyne (a), pentadeca-*trans*-2,*trans*-8,*cis*-10-triene-4,6-diyne (b), pentadeca-*trans*-2,*cis*-8,*trans*-10-4,6-diyne (c), and pentadeca-*trans*-2,*cis*-8,*cis*-10-triene-4,6-diyne (d). The origins of the electronic transitions are indicated (see text)

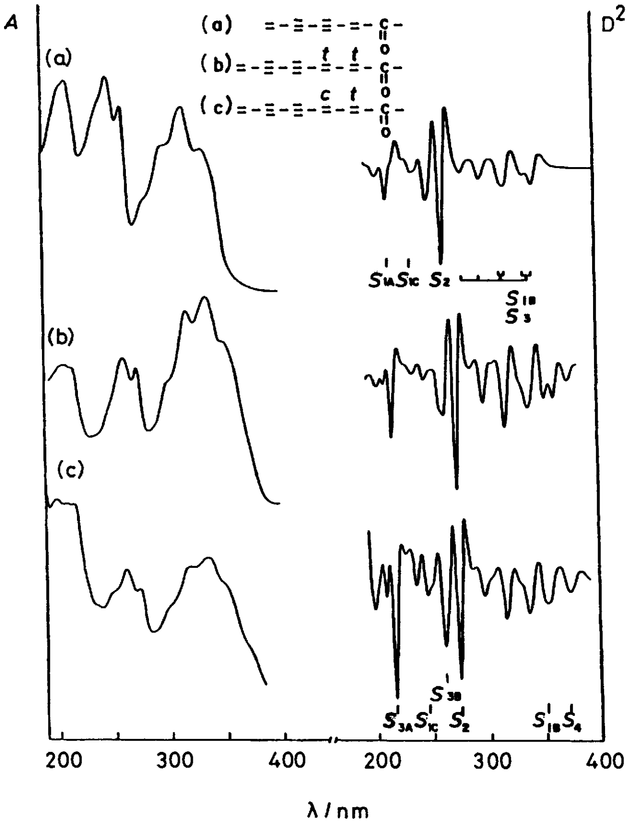

Figure 5. Absorption (left) and second-derivative (right) spectra of pentadeca-*trans*-2,*trans*-8-diene-4,6-diyn-10-one (a), pentadeca-*trans*-2,*trans*-8,*trans*-10-triene-4,6-diyn-12-one (b), and pentadeca-*trans*-2,*cis*-8, *trans*-10-triene-4,6-diyn-12-one (c). The origins of the electronic transitions are indicated (see text)

Weak bands, with maxima lying at positive D^2 values and at a wavelength intermediate between two strong bands, must be considered carefully. In fact they can be false peaks originating from the shape of two adjacent strong bands in the positive region. For instance the weak peaks alternating in the vibrational structure of the $\nu_{C\equiv C}$ mode might be due to an overlap contribution of a false peak and the ν_{C-C} stretching mode. It is possible to distinguish false from real peaks experimentally since the latter decrease their bandwidths as $\Delta\lambda$ is decreased. Anyway false peaks can never attain negative values.

We now discuss the spectra of the various compounds according to the order of the conjugating unsaturated groups.

System (**a**).—We have measured the absorption and D^2 spectra of compounds (**I**) (Figures 1 and 2) and (**II**) which exhibit two triple and a double carbon–carbon conjugated bonds. We expect three $\pi \longrightarrow \pi^*$ transitions, neglecting for the moment the acetylenic π bonds perpendicular to the plane of conjugation. The diacetylenic function 1 gives rise to two transitions, *via* exciton splitting, which, on the basis of local group C_{2h} pseudo-symmetry, belong to the irreducible representations A_g and B_u, respectively. The latter, which should correspond to coupling in phase $\overset{+}{C}\text{–}\overset{-}{C}\text{–}\overset{+}{C}\text{–}\overset{-}{C}$ of the local acetylenic transition moments, is strongly active. Its origin clearly occurs at 281 nm for compound (**I**). Its wavelength (265 nm) at the maximum agrees well with that observed (268 nm) for conjugated trienes and triynes. The vibrational peaks of this transition (S_0–S_{1B}) fit the series $\nu_{m,n}^{1B} = 35\,587 + 2\,140m + 1\,040n$ where m and n are integers with $m + n \leqslant 5$. The progressions are therefore due to the $\nu_{(C\equiv C)}$ and $\nu_{(C-C)}$ stretching modes (the occurrence of the latter mode should be regarded with caution, as discussed above), their overtones and combinations, the shift parameter $\Delta_{C\equiv C}$ being 1.6. The C≡C bond is much lengthened at the excited state as seen by the high value of the shift parameter as well as by the frequency reduction with respect to the ground state (2 250 cm^{-1}).

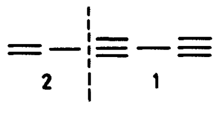

(a)

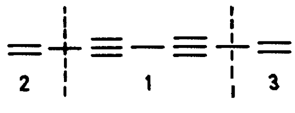

(b)

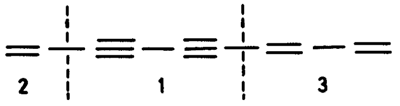

(c)

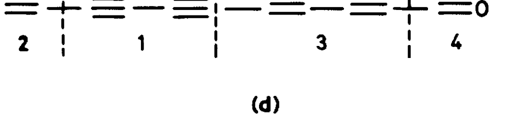

(d)

Similar frequencies for the origin and for the stretching modes as well as similar shift parameters have been found for compound (**II**) (Table). The electronic transition S_0–S_2 associated with the ethylenic group 2 clearly occurs at 211.5 nm for (**I**) [213.5 nm for (**II**)]. Its vibrational structure is not so well resolved as that discussed above and only three terms of the series $\nu_m^2 = 47\,281 + 1\,750m$ with $m \leqslant 2$ and $\Delta = 0.9$ are observed. The progression is essentially given by the $\nu_{(C=C)}$ stretching mode. However, its increased frequency (1 750 cm^{-1}) with respect to the ground state (1 650 cm^{-1}) indicates that the $\nu_{(C\equiv C)}$ stretching mode contributes to the envelope (see above) and another weak electronic transition overlaps. It should be the second transition of the A_g species (S_0–S_{1A}) of the diacetylenic group forbidden under the selection rules of the C_{2h} group, where the local acetylenic transition moments are coupled out of phase, $\overset{+}{C}\text{–}\overset{-}{C}\text{–}\overset{+}{C}\text{–}\overset{-}{C}$.

System (**b**).—In the spectra of compounds (**III**) and (**IV**) (Figure 2), which show four conjugated π bonds, the origin of the S_0–S_{1B} transition occurs at 311 [for (**III**)] and 314 [for (**IV**)] nm. The peaks of maximum intensity occur at 301 [(**III**)] and 303 [(**IV**)] nm which agree well with the absorption maxima of $H(CH{=}CH)_4H$ (304 nm) and $Me(C{\equiv}C)_4Me$ (306 nm). For both compounds the ν(C≡C) stretching mode is at 2 090 cm^{-1} with $\Delta = 1.7$. Clearly the C≡C bond is lengthened at the excited state more than for (**I**) and (**II**).

The second component of the exciton splitting, S_0–S_{1A}, occurs weakly at 203 nm with ν(C≡C) 2 000 cm^{-1}, Δ *ca.* 1 (see Table).

The two ethylenic bonds 2 and 3 should give rise to two accidental degenerate transitions S_0–S_2 and S_0–S_3. The two groups are sufficiently apart from each other, the resonance interaction being negligible, to give appreciable exciton splitting. Only a highly active transition is in fact observed at 247.5 nm ($\nu_{C=C}$ 1 700 cm^{-1}, Δ 1) for (**III**) and at 250 nm ($\nu_{C=C}$ 1 667 cm^{-1}, Δ 1.1) for (**IV**). The small differences between the

Table. Electronic transitions λ/nm and main terms of the vibrational progressions ν/cm^{-1}

Compound	$\underset{2}{=} \vdots \underset{1}{\equiv - \equiv} \vdots \underset{3}{= - =} \vdots \underset{4}{=}$	S_4		S_{1B}		S_2		S_{3B}		S_{1C}		S_{1A}		S_{3A}	
		λ	ν(C=O)	λ	ν(C≡C)	λ	ν(C=C)	λ	ν(C=C)	λ		λ	ν(C≡C)	λ	ν(C=C)
(I)	$= - \equiv - \equiv$			281	2 150	211.5	1 740								
(II)	$= - \equiv - \equiv - \quad -\mathrm{C}{=}\mathrm{O}$			282	2 130	213.5	1 700								
(III)	$= - \equiv - \equiv - = - \quad - \quad -\mathrm{C}{=}\mathrm{O}$			311	2 090	247.5	1 700			212		203	2 020		
(IV)	$= - \equiv - \equiv - = -\mathrm{C}-\mathrm{OH}$			314	2 090	250	1 670			217		204	2 000		
(V)	$= - \equiv - \equiv - \overset{t}{=} - \overset{t}{=}$			334	2 060	265	1 630	246	1 720	228	1 180	210	1 850	210	1 850[a]
(VI)	$= - \equiv - \equiv - \overset{t}{\equiv} - \overset{t}{\equiv} -\mathrm{C}-\mathrm{OH}$			336	2 030	266.5	1 600	249		235	1 310	215	1 800	215	1 800[a]
(VII)	$= - \equiv - \equiv - \overset{t}{=} - \overset{c}{=}$			336	2 030	266	1 540	251	1 480	227	1 400	213	1 830	213	1 830[a]
(VIII)	$= - \equiv - \equiv - \overset{c}{=} - \overset{t}{=}$			333	2 070	265	1 790	246	1 550	227	1 400			211	1 630
(IX)	$= - \equiv - \equiv - \overset{c}{=} - \overset{t}{=} -\mathrm{C}-\mathrm{OH}$			335	2 040	267		249	1 600	230	1 365	215	1 800	215	1 800[a]
(X)	$= - \equiv - \equiv - \overset{c}{=} - \overset{c}{=}$			336	2 080	266	1 780	250	1 500	229	1 580			212	1 610
(XI)	$= - \equiv - \equiv - = -\mathrm{C}{=}\mathrm{O}$			339[b]	2 150	262	2 150[c]			235	1 690	211	2 110		
(XII)	$= - \equiv - \equiv - \overset{t}{=} - \overset{t}{=} -\mathrm{C}{=}\mathrm{O}$	373	1 600	360	2 000	273	1 540	258		244	1 750			216	1 550
(XIII)	$= - \equiv - \equiv - \overset{c}{=} - \overset{t}{=} -\mathrm{C}{=}\mathrm{O}$	373	≃1 600		2 000[d]	274		261	1 690	247				216	1 550

[a] Overlap with the S_0–S_{1A} transition. [b] Value corresponding to the centre of the doublet (336—343 nm) due to configurational interaction between S_0–S_{1B} and S_0–S_3. [c] The high value of the vibrational term is due to configurational interaction. [d] The origin overlaps with the 0—1 term of the S_4 transition. The vibrational spacing is obtained from the higher terms of the progression.

two compounds in the electronic and vibrational frequencies should be attributed to the inductive effect of the adjacent hydroxy group. Although all four expected $\pi \longrightarrow \pi^*$ transitions due to the four conjugated unsaturated groups have been *localized in* both spectra, an additional weak band appears at 212 nm for **(III)** [217 nm for **(IV)**] which does not show appreciable vibrational structure. We tentatively assign this band to the S_0–S_{1C} transition, *i.e.* to the $\pi \longrightarrow \pi^*$ diacetylenic transition in the plane perpendicular to the conjugation plane. In this case the C≡C and C–C bond lengths should not be much affected by the electronic excitation. Therefore the corresponding shift parameters are small.

System (**c**).—The spectra of seven compounds **(V)**—**(XI)** with five conjugated π bonds, exhibiting different *cis–trans* configurations at the butadiene group 3 have been measured. The absorption and D^2 spectra of **(V)**, **(VII)**, **(VIII)**, and **(X)** are shown in Figure 3. Apart from the carbonyl derivative **(XI)** (see below) the spectra of the compounds show a strong S_0–S_{1B} transition at 334—336 nm [334 nm for $H(CH{=}CH)_5H$] with $\nu_{C\equiv C}$ *ca.* 2 050 cm^{-1} and Δ *ca.* 1.8. Compounds **(V)**, **(VI)**, and **(IX)** show also the ν(C–C) progression as a shoulder (Table). Therefore the lengthening of the triple bond upon excitation is more pronounced than for the chromophores with four π bonds.

The S_0–S_2 transition of the ethylenic group 2 shifts further to 265 nm; its vibrational structure involves the double bond (Table).

Combined spectral analysis of compounds **(V)** (*trans–trans* at group 3), **(VII)** (*trans–cis*), **(VIII)** (*cis–trans*), and **(X)** (*cis–cis*) furnishes the assignment of other transitions together with a clear example of a *cis*-effect previously discussed.[18,19] The S_0–S_{3B} transition of the butadiene group 3 is assigned to the band system with origin at 250 nm. Its S_0–S_{3A} counterpart should occur in the 200—220 nm region, close to the S_0–S_{1A} transition of the acetylenic group 1. The band system at 210—215 nm is weak for compounds **(V)** (*trans–trans*) and **(VII)** (*trans–cis*) and rather strong for compounds **(VIII)** (*cis–trans*) and **(X)** (*cis–cis*). In addition the vibrational structure is clearly due to the double carbon–carbon bond for the latter pair [1 630 for **(VIII)** and 1 610 cm^{-1} for **(X)**], while it has intermediate character between the double and the triple bond for **(V)** (1 850 cm^{-1}) and **(VII)** (1 830 cm^{-1}). Clearly the S_0–S_{1A} and S_0–S_{3A} transitions overlap, the latter being here intense for the *cis*-compounds. The relative intensities of the transitions are easily interpreted in terms of the relative distortions from the C_{2h} pseudo-symmetry. Coupling between the transition moments of the ethylenic groups gives rise to the two transitions, S_0–S_{3A} and the S_0–S_{3B}, the first being weaker because of out-of-phase coupling (forbidden for the C_{2h} group). For the *trans*-compounds the two S_0–S_3 transitions are expected to be weak because of their opposite moments to the S_0–S_{1B} transition. For the *cis*-compounds the S_0–S_3 transition moments develop at a large angle to the S_0–S_1 transition moments. Therefore both bands at 210 and 250 nm in the *cis*-compounds are enhanced in intensity, showing the vibrational structure involving the double bond, with respect to the corresponding bands of the *trans*-compounds. Analogous effects are observed for the corresponding *trans–trans* **(VI)** and *cis–trans* **(IX)** hydroxy derivatives. For both cases, probably due to inductive effects, the S_0–S_{1A} transition is rather intense. In fact the vibrational structure of the short wavelength band has intermediate character between triple and double bonds.

The spectrum of the carbonyl derivative **(XI)** with five conjugated unsaturated groups shows interesting features (Figure 4). The bands due to the butadiene group 3 disappear, being replaced by transitions localized on the C=C and C=O groups. One occurs at 235 nm, its vibrational pattern corresponding to the double bond. Therefore the band at 211 nm is due solely to the S_0–S_{1A} transition, showing the vibrational progression of the triple bond (2 100 cm^{-1}). The other localized exciton at the double bond gives rise to accidental degeneracy with the S_0–S_{1B} transition causing pronounced configurational interaction. In fact the vibrational progression of the two transitions cannot be ordered separately. The right spacings between the origin and the overtones are found only by taking the centre of gravity (339, 316, and 296 nm) of the doublets at 343—336, 318—315, and 296 nm. It is seen (Figure 4) that the value of the splitting decreases on going from the origin to the higher overtones. Configurational interaction manifests itself also in the high wavelength of the S_0–S_{1B} transition (343 nm compared with 335 nm for the other compound) as well as in the vibrational pattern of the S_0–S_2 transition at 262 nm which shows spacings of 2 100 cm^{-1}. Clearly for this compound the cumulene resonance structure stabilizes the excited state, all three lowest lying transitions exhibiting vibrational progressions of *ca.* 2 000 cm^{-1} which correspond to the frequency of the C=C=C stretching mode of allene.

System (**d**).—For compounds **(XII)** and **(XIII)** (Figure 4) the origin of the S_0–S_{1B} transition is shifted to 360 nm corresponding to the lowest transition (364 nm) of the polyene $H(CH{=}CH)_6H$. For these cases this transition does not coincide with the 'C=O double bond' transition which is observed at 373 nm with 1 600 cm^{-1} vibrational spacing. No evidence for interaction between the two transitions is found. In fact the S_0–S_2 transition at 273 nm shows the characteristic double-bond vibrational structure. The S_0–S_{3A} and S_0–S_{3B} transitions of the butadiene group 3 occur at 216 and 260 nm, respectively, being enhanced for the *cis–trans* compound **(XIII)** with respect to the *trans–trans* compound **(XII)**. Both transitions of both compounds shows the vibrational pattern of the double bond.

Conclusions.—The analysis of the vibrational structure regarding both frequencies and relative intensities, at the moderate resolution allowed by measurement of the second-derivative spectra, permits the electronic transitions to be characterized. These are well interpreted in terms of localized excitations at the π bonds. The assignment of the various electronic transitions is confirmed, on a correlative basis, by spectral measurements on a series of compounds with slightly different local chromophores in different conformations. This allowed us to demonstrate and interpret in terms of localized excitons the *cis*-effect previously described.

These results account for all the structural characteristics, stereoisomerism included, of a certain sequence of triple and double bonds, providing a complete fingerprint of the polyacetylene chromophores and a new tool for routine identification of naturally occurring polyacetylenes.[20]

Acknowledgements

This work was supported by the Italian Ministero della Pubblica Istruzione.

References

1 B. S. Hudson, B. E. Kohler, and K. Schulten, 'Excited States,' ed. E. C. Lim, Academic Press, New York, 1982, vol. 6, pp. 1—95 and references therein.
2 W. Drenth and E. H. Wiebenga, *Acta Crystallogr.*, 1955, **8**, 755.
3 J. R. Platt, *J. Chem. Phys.*, 1956, **25**, 80.
4 W. J. Campion and M. Karplus, *Mol. Phys.*, 1973, **25**, 30.
5 D. Pugh, *Mol. Phys.*, 1973, **26**, 1297.
6 C. Tric and O. Parodi, *Mol. Phys.*, 1967, **13**, 1.
7 J. A. Pople and S. H. Walmsley, *Trans. Faraday Soc.*, 1962, **58**, 441.
8 H. C. Longuet-Higgins and J. N. Murrell, *Proc. Phys. Soc. A*, 1953, **68**, 601.

9 W. T. Simpson, *J. Am. Chem. Soc.*, 1955, **77**, 6164.
10 K. Schulten and M. Karplus, *Chem. Phys. Lett.*, 1972, **14**, 305.
11 F. F. Vincieri, S. A. Coran, V. Giannelini, and M. Bambagiotti Alberti, *Chem. Ber.*, 1981, **114**, 486.
12 F. F. Vincieri, S. A. Coran, V. Giannellini, and M. Bambagiotti Alberti, *Planta Med.*, 1985, **81**, 107.
13 F. Bohlmann, T. Burkhardt, and C. Zdero, 'Naturally Occurring Acetylenes,' Academic Press, London, 1973.
14 H. H. Jaffé and M. Orchin, 'Theory and Applications of Ultraviolet Spectroscopy,' Wiley, New York, 1962, pp. 228—239.
15 A. B. Myers, R. A. Mathies, D. J. Tannor, and E. J. Teller, *J. Chem. Phys.*, 1982, **77**, 3857.
16 R. M. Gavin, Jr., C. Weisman, J. K. McVey, and S. A. Rice, *J. Chem. Phys.*, 1978, **68**, 522.
17 G. Smulevich, A. Amirav, U. Even, and J. Jortner, *Chem. Phys.*, 1982, **73**, 1.
18 A. Sandoval and L. Zechmeister, *J. Am. Chem. Soc.*, 1947, **69**, 553.
19 T. H. Pinckard, B. Willie, and H. Zechmeister, *J. Am. Chem. Soc.*, 1948, **70**, 1938.
20 F. F. Vincieri, S. A. Coran, M. Bambagiotti Alberti, G. Smulevich, and M. P. Marzocchi, *Chem. Ber.*, 1986, **119**, 2843.

Received 24th July 1986; *Paper* 6/1509